JACS
JOURNAL OF THE AMERICAN CHEMICAL SOCIETY

Article

pubs.acs.org/JACS

Tunable Heptamethine–Azo Dye Conjugate as an NIR Fluorescent Probe for the Selective Detection of Mitochondrial Glutathione over Cysteine and Homocysteine

Soo-Yeon Lim,[†] Keum-Hee Hong,[†] Dae Il Kim,[‡] Hyockman Kwon,[‡] and Hae-Jo Kim*[,†]

[†]Department of Chemistry, Hankuk University of Foreign Studies, Yongin 449-791, Republic of Korea

[‡]Department of Bioscience and Biotechnology, Hankuk University of Foreign Studies, Yongin 449-791, Republic of Korea

Supporting Information

ABSTRACT: Although a lot of mitochondria-targeting biothiol probes have been developed and applied to cellular imaging through thiol-induced disulfide cleavage or Michael addition reactions, relatively few probes assess mitochondrial GSH with high selectivity over Cys and Hcy and with NIR fluorescence capable of noninvasive imaging in biological samples. In order to monitor mitochondrial GSH with low background autofluorescence, we designed a heptamethine–azo conjugate as an NIR fluorescent probe by introducing a tunable lipophilic cation unit as the biomarker for mitochondria and a nitroazo group as the GSH-selective reaction site as well as the fluorescence quencher. The probe exhibited a dramatic off–on NIR fluorescence response toward GSH with high selectivity over other amino acids including Cys and Hcy. Further application to cellular imaging indicated that the probe was highly responsive to the changes of mitochondrial GSH in cells.

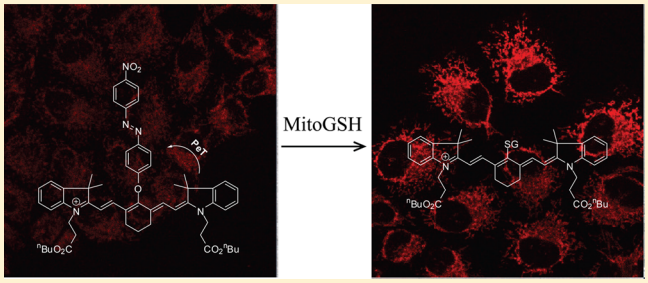

INTRODUCTION

Mitochondrion is an essential organelle within eukaryotic cells, utilizing oxygen to digest carbohydrates and fats and releasing reactive oxygen species (ROS) as well as biochemical energy in the form of adenosine triphosphate. In addition, mitochondria are also involved in the event of ROS-induced apoptosis. Due to these crucial functions, oxidative damage to the mitochondria is a significant factor on cell death which underlies many neurodegenerative diseases and pathologies. In order to protect cells from the oxidative stress, mitochondria are equipped with a number of free radical scavengers and the mitochondrial glutathione (γ-glutamylcysteinylglycine or GSH) pool is a critical antioxidant reservoir within cells.[1] Therefore, it is a challenge to develop a mitochondrial GSH probe and to apply it for the detection of the level of mitochondrial GSH in cells.

In spite of the remarkable advances in the design of fluorescent probes for biothiols[2] including Cys and Hcy[3] over the past decade, relatively few probes have been developed that exhibit a selective fluorescence response to mitochondrial GSH.[4] Most of them, including the triphenylphosphonium-appended disulfide fluorophore and the commercially available monochlorobimane (mCB), cannot discriminate GSH from Cys or Hcy due to the functional similarity of those biothiols. Recently, a pioneering work by Yang and his co-workers showed that a BODIPY-based probe could produce a highly selective and ratiometric fluorescence change with GSH relative to Cys and Hcy.[4a] The probe, if treated with Cys or Hcy, formed an initial thioether and subsequently underwent a rearrangement reaction to produce the thermodynamically stable amino-substituted BODIPY complex, whereas the probe formed a thioether type of BODIPY complex with GSH and produced a strong fluorescence at 588 nm. Strongin and his co-workers reported another interesting micelle-mediated GSH probe, which displayed a GSH selective green fluorescence in the presence of cationic micelles.[4b] Abliz and his co-workers also devised a reversible fluorescent sensor, which was successfully applied for selective intracellular imaging of GSH.[4c] However, these GSH-selective probes were limited in their ability to target mitochondria.

Until now, few fluorescent probes were available to target mitochondrial GSH with NIR fluorescence, which is more desirable for noninvasive *in vivo* imaging of mitochondrion-related diseases without interfering with cellular autofluorescence. Herein we report a heptamethine–azo dye conjugate (**MitoGP**), where the tunable lipophilic cation of a heptamethine unit was utilized as the mitochondrial biomarker and a nitroazo group was introduced as the GSH-selective reaction unit as well as the fluorescence quencher. In the presence of GSH, **MitoGP** exhibited a dramatic fluorescence off–on response at λ_{max} 810 nm, while the other amino acids including Cys and Hcy displayed no significant NIR fluorescence relative to GSH. Cellular imaging experiments

Received: January 28, 2014
Published: April 23, 2014

 © 2014 American Chemical Society dx.doi.org/10.1021/ja500962u | *J. Am. Chem. Soc.* 2014, 136, 7018–7025

clearly indicated that the fluorescence was well reflected by the changes of GSH concentration in mitochondria.

RESULTS AND DISCUSSION

Design and Synthesis of MitoGP. To target mitochondrial GSH with a high signal-to-noise (S/N) ratio, we designed an NIR fluorophore (**MitoGP**) by employing both the mitochondria-targetable site with a tunable cationic heptamethine unit and the GSH-activatable site with a labile nitroazo aryl ether group (Scheme 1). The nitroazo ether group was introduced as the GSH-selective reaction unit as well as the fluorescence quencher unit. Through a plausible substitution reaction of the azo group with GSH, the probe was expected to significantly enhance the fluorescence of **MitoGP**. The mitochondrial GSH probe was effectively prepared from heptamethine chloride (**1**) and nitroazo phenol (**2**) (Scheme 2). The precursor, heptamethine chloride (**1**) was readily available according to a modified procedure previously described in the literature.[5] The analogues of **MitoGP** (**3**, **4**) were synthesized through hydrolysis of **MitoGP** and subsequent amide coupling, respectively, in order to investigate the effect of the tunable functionality of **MitoGP** on quantum yields and cellular distribution.

Scheme 1. Design of an NIR-Based Mitochondrial GSH Probe

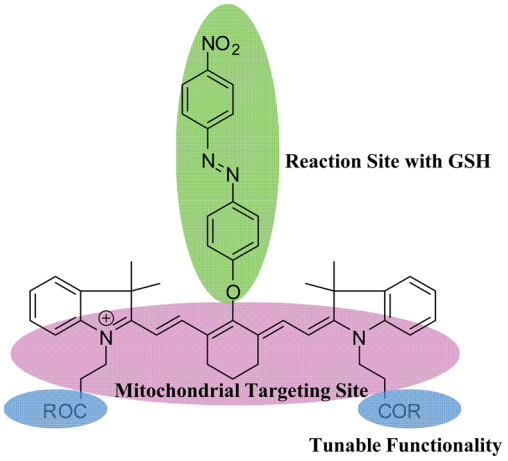

Reaction Kinetics. The addition of GSH (10 mM) to **MitoGP** (10 μM in HEPES buffer, 0.10 M, pH 7.4) induced a typical ratiometric change with two isosbestic points at 600 and 824 nm in UV−vis spectra, whose kinetic analysis gave the second-order rate constant of k 0.062 ($\pm$0.005) M^{-1} s^{-1} at 25 °C. The fluorescence spectra of **MitoGP** displayed a remarkable red-shift (λ_{em} 764 to 810 nm) in its maximum wavelength with a dramatic increase in the intensity at λ_{max} 810 nm upon addition of GSH (Figure 1). The quantum yield of **MitoGP** was measured in the absence and presence of GSH, using IR-820 as a reference compound,[6] resulted in Φ 0.0011 and 0.187 for **MitoGP** and **MitoGP**−GSH, respectively. As expected, the initial quantum yield of **MitoGP** was quite low due to the quenching effect of a nitroazo group of **MitoGP** through a probable photoinduced electron transfer (PeT) from cyanine to the nitroazo group. However, reaction of **MitoGP** with GSH resulted in a significantly larger value that was as high

Scheme 2. Synthesis of a Mitochondrial GSH Probe (MitoGP) and Its Analogues

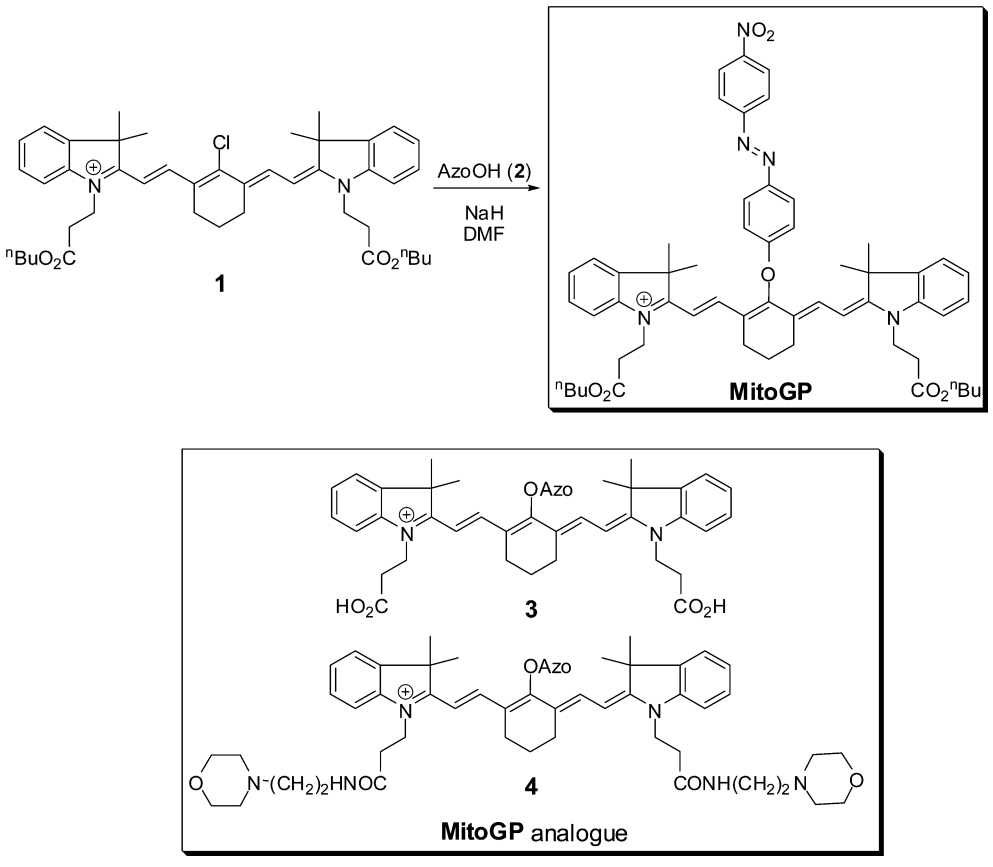

dx.doi.org/10.1021/ja500962u | J. Am. Chem. Soc. 2014, 136, 7018−7025

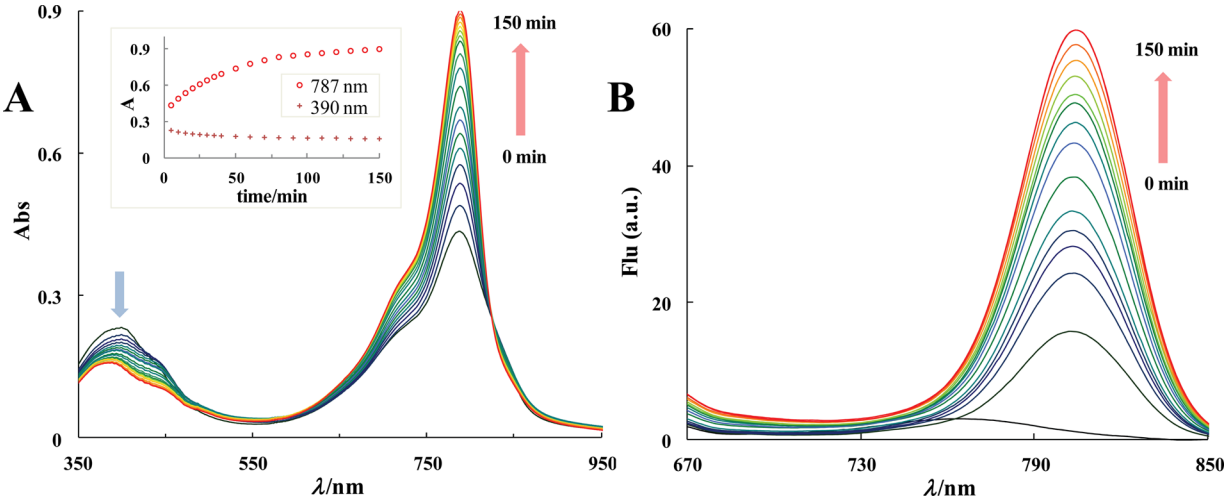

Figure 1. Time-dependent UV–vis (A) and fluorescence (B) spectra of **MitoGP** (10 μM, ex 600 nm) upon addition of GSH (10 mM) in HEPES buffer (0.10 M, pH 7.4). Inset: UV–vis kinetics.

as Φ 0.187 (**MitoGP**–GSH). This dramatic fluorescence turn-on effect is one of the advantages of **MitoGP** compared to the other cyanine-based NIR dye such as control compound **1** (Φ 0.022), where the inherent fluorescence was relatively strong compared to **MitoGP** (Table 1).[7] The analogues **3** and **4** also

Table 1. Spectroscopic Properties of MitoGP and Its Analogues[a]

entry	cmpd	max. λ_{abs}/nm	$\varepsilon/10^5$ M^{-1} cm^{-1}	max. λ_{em}/nm	Φ (%)
1	**1**	780	0.20	790	2.16
2	**MitoGP**	790	0.43	764	0.11
3	**3**	755	0.61	776	5.59
4	**4**	770	0.69	775	4.06
5	**MitoGP**–GSH[b]	787	1.01	810	18.7

[a]Spectral measurements were performed in HEPES buffer (0.10 M, pH 7.4) by using IR-820 as a reference compound. [b]Spectral data of the complex between **MitoGP** and GSH was measured 12 h after addition of 10 mM of GSH in HEPES buffer (0.10 M, pH 7.4).

exhibited strong intrinsic fluorescence with Φ 0.056 and 0.041, respectively, at wavelengths similar to that of **MitoGP**. The strong fluorescence of the analogues and compound **1** was not likely to increase the *S*/*N* ratio for cellular imaging. We, therefore, expected that **MitoGP** would be a good candidate as an imaging probe for mitochondrial GSH in cells.

GSH Selectivity. The GSH selectivity of **MitoGP** in HEPES buffer (0.10 M, pH 7.4) was measured for various amino acids (AAs) including Cys and Hcy. **MitoGP** did not produce any detectable fluorescence without GSH (F_0 = 0.138 at λ_{max} 810 nm) but the addition of GSH induced a dramatic fluorescence increase with F/F_0 460 at λ_{max} 810 nm (Figure 2A). Interestingly, Cys and Hcy showed weak and blue-shifted fluorescence responses at λ_{max} 747 nm[8] but their fluorescence enhancement was very weak compared to GSH: F/F_0 10 and 15 for Cys and Hcy, respectively. In addition, competitive fluorescence assay showed that most AAs did not exhibit any interference with GSH unlike Cys and Hcy (Figure 2B). Cys or Hcy might form stable amino-substituted covalent complexes with **MitoGP** through a sequential thiol substitution and rearrangement reaction as observed in Yang's BODIPY-based probe.[4a] We observed that the initial thioether underwent a

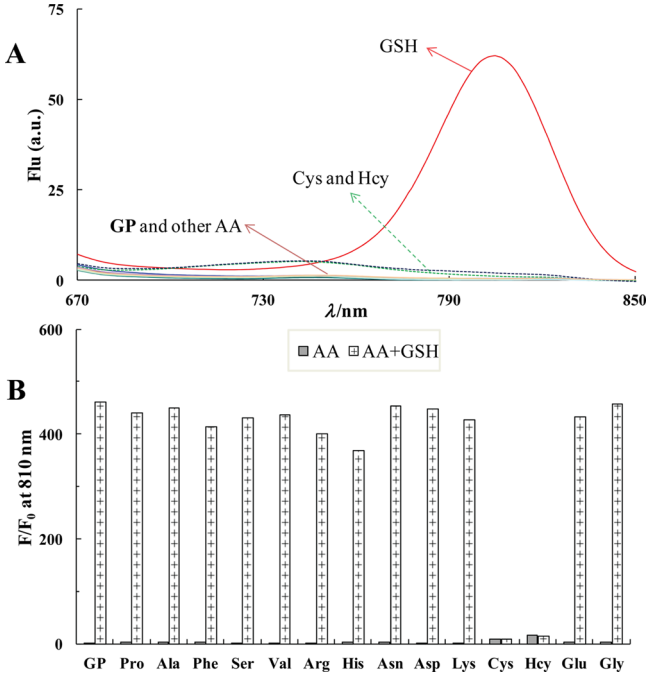

Figure 2. (A) Fluorescence response of **MitoGP** (10 μM, λ_{ex} 600 nm) with various AAs, GSH, Cys and Hcy (10 mM, 3 h) in HEPES buffer (0.10 M, pH 7.4). (B) The competitive assay of GSH against **MitoGP** + AA: Black columns for **MitoGP** + AA, cross bar columns for **MitoGP** + AA + GSH. F_0 is the fluorescence intensity of **MitoGP** alone at λ 810 nm.

subsequent intramolecular amination reaction (Figure S15 in the Supporting Information [SI]), which induced a blue shift in the fluorescence spectra of low intensity associated with Cys/Hcy (Figure S16 in the SI). The competitive experiments indicated that **MitoGP** was so selective toward GSH that its fluorescence was dramatically turned on by GSH.

NMR Spectral Analysis. To gain insight into the reaction mechanism of **MitoGP** with GSH, we performed ^{1}H NMR spectral analysis of **MitoGP** in the presence of 2-mercaptoethanol (ME), an organic soluble analogue of GSH. Upon addition of ME in methanol-d_4, the spectrum of **MitoGP** was slowly converted into another discrete set of **MitoGP**–ME. In

dx.doi.org/10.1021/ja500962u | J. Am. Chem. Soc. 2014, 136, 7018–7025

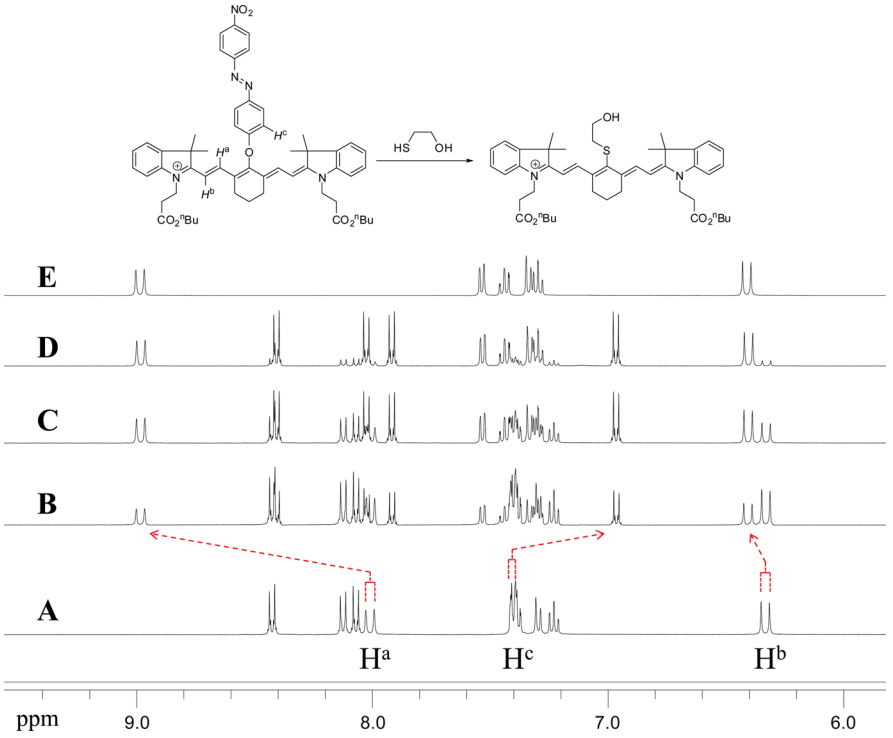

Figure 3. Partial ^{1}H NMR spectra of **MitoGP** (10 mM) in the presence of ME (1.2 equiv) in CD_3OD. (A) **MitoGP**, (B) 0.5 h after addition of ME, (C) 2 h, (D) 12 h, (E) **MitoGP**−ME.

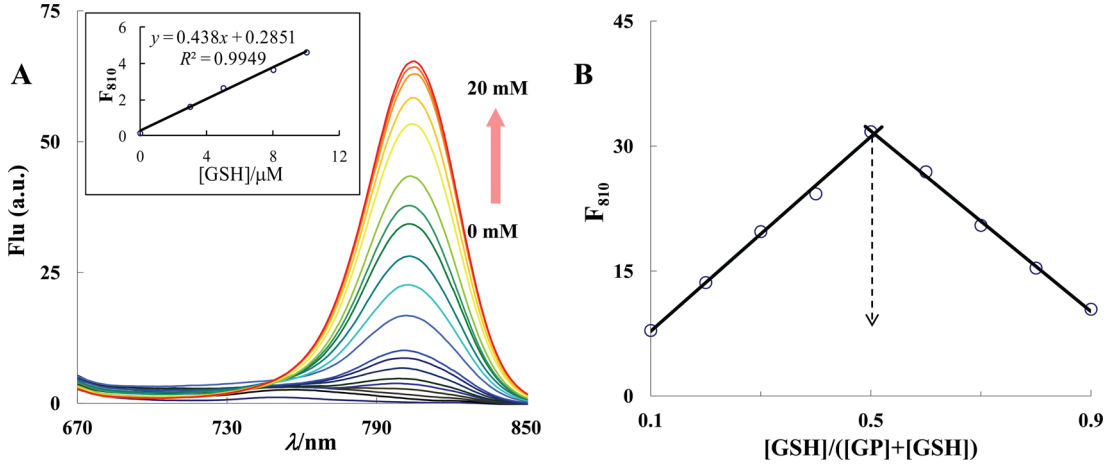

Figure 4. (A) Fluorescence changes of **MitoGP** (10 μM, λ_{ex} 600 nm) on the incremental addition of GSH in HEPES buffer (0.10 M, pH 7.4); (inset) linear plot of the fluorescence intensity of **MitoGP** against GSH. (B) Job's plot between **MitoGP** ($\lambda_{ex}/\lambda_{em}$ 600/810 nm) and GSH. Total concentrations of **MitoGP** and GSH were kept constant at 10 mM during incubation (3 h) and then diluted with HEPES buffer (0.10 M, pH 7.4) to measure their fluorescence intensities.

the presence of 1 equiv ME, the vinylic protons of **MitoGP** were dramatically shifted to downfield regions (H^a 8.01 to 8.98 ppm, H^b 6.33 to 6.40 ppm) while the nitroazo aryl ether proton of **MitoGP** was shifted to an upfield region (H^c 7.40 ppm to 6.97 ppm) owing to the release of free nitroazophenol. The product structure was confirmed by an authentic **MitoGP**−ME compound (Figure 3). The spectral changes indicated that the azophenol of **MitoGP** was easily substituted with a thiol group, which produced a dramatic change in the fluorescence. When treated with 0.50 equiv of Cys, however, **MitoGP** was converted from the initial thioether into a stable amine structure through a rearrangement reaction that resulted in a stable 2:1 complex between **MitoGP** and Cys visible in the ^{1}H NMR and mass spectra (Figures S15 and S13 in the SI).[9]

Limit of Detection and Reaction Stoichiometry. The limit of detection of GSH was measured with **MitoGP** (10 μM) by incremental addition of GSH in HEPES buffer (0.1 M, pH 7.4) (Figure 4A). The fluorescence intensity of **MitoGP** gradually increased according to the amount of GSH added and eventually saturated at 10 mM GSH (Figure S14 in the SI). From the linear range of the titration plot, the detection limit of GSH was determined to be as low as 26 nM at $3\sigma/m$, where σ is the standard deviation of blank measurements of **MitoGP** and m is the slope obtained from the linear plot of **MitoGP** fluorescence against GSH (Figure 4A, inset).

dx.doi.org/10.1021/ja500962u | J. Am. Chem. Soc. 2014, 136, 7018−7025

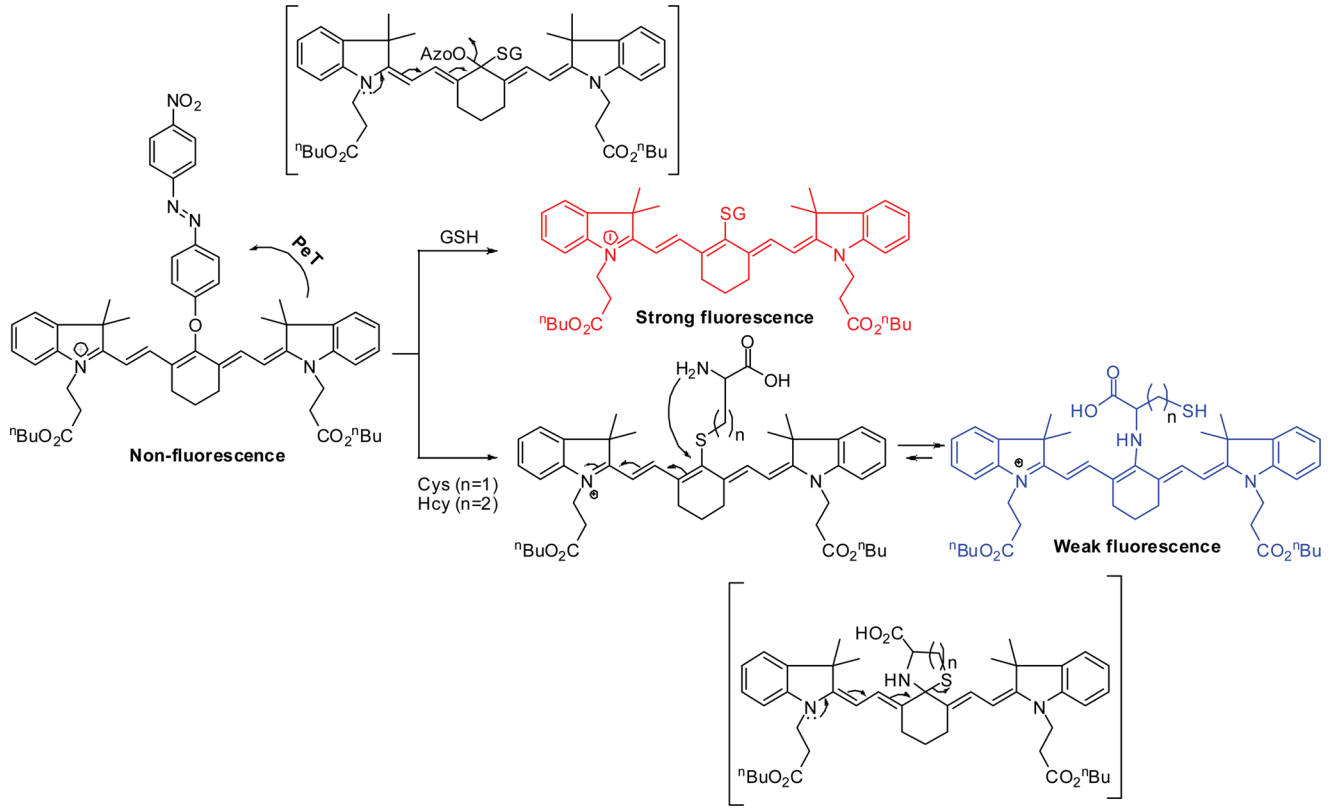

Figure 5. Proposed reaction mechanism of **MitoGP** with GSH vs Cys/Hcy.

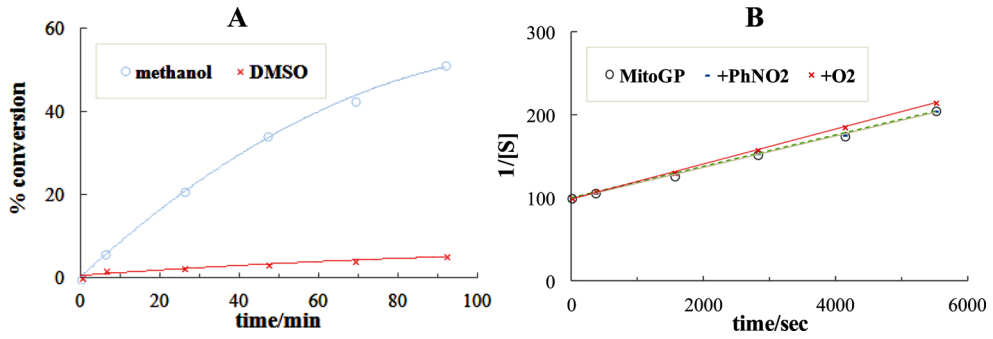

Figure 6. Reaction profile of **MitoGP** with ME (both 10 mM) in different solvents (A) and in the presence of radical/electron scavengers (B). The reaction was measured by ^{1}H NMR spectral analysis.

The reaction ratio of **MitoGP** was precisely determined using the Job's plot. The fluorescence intensity of **MitoGP** at 810 nm reached the maximum value when the mole fraction of GSH was 0.5, indicating that one-to-one reaction took place between **MitoGP** and GSH (Figure 4B).

Further pH-dependent fluorescence measurement showed that **MitoGP**−GSH complex displayed a strong fluorescence at 810 nm with a stable pH profile between 6 and 9, whereas **MitoGP** exhibited negligible fluorescence over a wide range of pHs (Figure S17 in the SI).

Mechanistic Study. From the combined results of UV−vis, fluorescence, and NMR spectral data, we propose the reaction mechanism of **MitoGP** with GSH in water. The initial **MitoGP** is nonfluorescent due to a possible photoinduced electron transfer (PeT) from indocyanine to a nitroazo group[10] and, furthermore, due to the soluble aggregate formation such as vesicles or micelles in an aqueous buffer.[11] The labile nitroazo group was rapidly replaced by the 1,6-conjugate addition of an alkyl thiol group of anionic GSH to the vinyl analogue of a cationic aza Michael acceptor.[12] The subsequent elimination reaction produced strong fluorescence on the probe (Figure 5).

A radical nucleophilic substitution ($S_{RN}1$) mechanism through an initial single-electron transfer from the nucleophilic thiol is also another possible explanation for the substitution in organic solvents.[13] However, we observed that the reaction rate of **MitoGP** with GSH was severely affected by the solvents used (Figure 6A), which would be implausible with a neutral radical mechanism. For example, the rate was accelerated more than 10 times in protic solvent (methanol) than aprotic solvent (DMSO). Furthermore, introduction of molecular oxygen (O_2), a radical scavenger, or nitrobenzene ($PhNO_2$), an electron scavenger, did not significantly alter the reaction rates of **MitoGP** to ME: the second-order reaction kinetics measured at 25 °C in ^{1}H NMR spectroscopy gave the rate constants (k) as 0.0189(±0.0042), 0.0208(±0.0022), and 0.0189(±0.0024) M^{-1} s^{-1} for **MitoGP** alone, **MitoGP**+O_2,

dx.doi.org/10.1021/ja500962u | J. Am. Chem. Soc. 2014, 136, 7018−7025

and **MitoGP**+$PhNO_2$, respectively (Figure 6B). Consequently, the thiol substitution reaction was likely to proceed through the nucleophilic addition and elimination mechanism instead of the radical substitution mechanism, at least in the protic solvent.

It is remarkable that neutral Cys and Hcy underwent relatively a slow addition reaction with cationic **MitoGP** and further rearrangement reaction with the neighboring amino group created the amino substituted cyanine dyes, which were thermodynamically stable and resistant to the nucleophilic substitution reaction of the second GSH as observed in the competitive reaction of **MitoGP**−Cys and **MitoGP**−Hcy against GSH. The resulting amino-substituted cyanine dyes provoked smaller changes in the fluorescence intensity than the thiol-substituted probe (**MitoGP**−GSH), which was the key contributor for discrimination of GSH from Cys and Hcy.

Role of Tunable Functional Group. We found that the butyl ester functional group of **MitoGP** is very important for the selective recognition and reaction kinetics of GSH in mitochondria compared to that of carboxylic acid or amide. While the cationic **MitoGP** was a good fluorescent probe for mitochondrial GSH with a high S/N ratio as well as a reasonable reaction rate, its acid analogue **3** was a poor probe with a low S/N ratio for GSH and exhibited a very sluggish reaction with GSH due to the electrostatic repulsion between GSH and the negatively charged **3** (Figure S18 in the SI). The amide analogue (**4**) showed almost a similar reaction rate as **MitoGP** with a biothiol but its S/N ratio was not as good as that of **MitoGP**. Furthermore, the analogues **3** and **4**, unlike **MitoGP**, were designed to target the biothiols in cytosol and lysosome, respectively. We anticipate that the probe will be extendable as organelle-specific dyes by changing the tunable functionality at the position of the ester group of the probe, which is currently in progress.

Cellular Imaging. Owing to the favorable biocompatible attributes of **MitoGP**, we performed a cellular imaging experiment of **MitoGP** under the confocal laser scanning microscope. Colocalization study of **MitoGP** with a green fluorescent mitochondrial tracker (rhodamine 123) clearly showed that cellular mitochondria was effectively stainable with 1.0 μM of **MitoGP** and displayed a strong fluorescence whose efficiency was comparable with that of the commercial MitoTracker (Figure 7).

If a mitochondrial specific enzyme (3-hydroxybutanoate dehydrogenase)-related GSH scavenger such as 3-hydroxy-4-pentenoate (3-HP, 1 mM, 5 min)[14] or 3-oxo-4-pentenoate (3-OP, 1 mM, 10 min)[15] was applied prior to the administration of **MitoGP** to HeLa cells, the fluorescence intensity was significantly decreased. The degree of the fluorescence decrease was dependent on the incubation time and the amount of the scavenger (Figure 8). While the fluorescence intensity of **MitoGP** was significantly reduced as much as 52% of the original intensity by the pretreatment of 3-HP (1 mM, 5 min and then incubation for 2 h), the cellular pretreatment with α-lipoic acid (LPA, a GSH enhancer, 1.8 mM, 24 h)[16] induced an approximately 1.5-fold increase in the fluorescence intensity relative to **MitoGP** alone (Figure 9). These cellular experiments indicated that the fluorescence intensity of **MitoGP** was well reflected on the levels of GSH in mitochondria and that **MitoGP** is a good fluorescent indicator for mitochondrial GSH in cells.

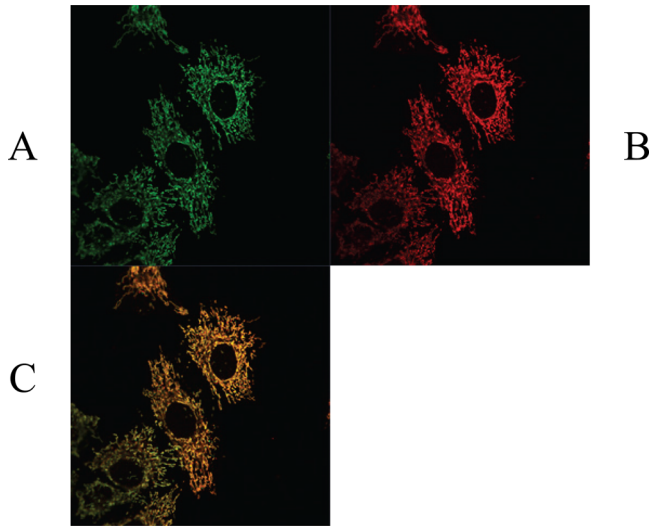

Figure 7. Confocal laser scanning microscopic images of **MitoGP** and rhodamine 123 in living HeLa cells. (A) Rhodamine 123 (1.0 μM, 15 min, λ_{ex} 488 nm). (B) **MitoGP** (1.0 μM, 30 min, λ_{ex} 555 nm). (C) Colocalization of the cells with the mitochondrial tracker and **MitoGP**. Colocalization coefficient between rhodamine 123 and **MitoGP** was analyzed by the implemented ZEN software to be 0.93 (0: no colocalization, 1: colocalization in all pixels).

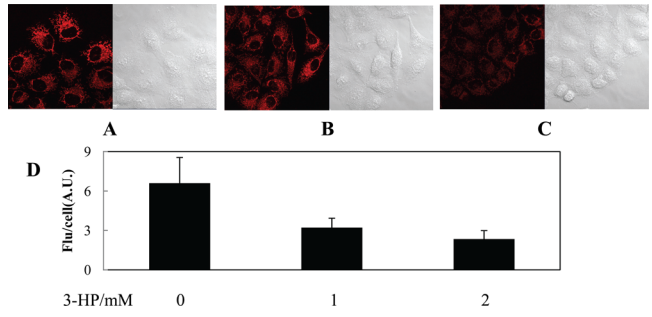

Figure 8. Confocal laser scanning microscopic images of **MitoGP** (2.0 μM, 30 min, λ_{ex} 555 nm) in the presence of a mitochondrial GSH scavenger (3-HP). (A) **MitoGP** only, (B) **MitoGP** + 3-HP (1 mM, 5 min, then 2 h incubation), (C) **MitoGP** + 3-HP (1 mM, 5 min, then 4 h incubation), (D) 3-HP concentration-dependent fluorescence of **MitoGP** (3-HP for 5 min, then 2 h incubation).

■ CONCLUSION

We designed a novel off−on mitochondrial GSH probe (**MitoGP**) by introduction of both the mitochondria-targeting site and the GSH reaction site to the backbone of a tunable NIR heptamethine probe. The initial nitroazo probe was nonfluorescent, but the reaction of **MitoGP** with GSH resulted in a dramatic increase in the NIR fluorescence with a high selectivity toward GSH over Cys/Hcy. The heptamethine−azo conjugate was successfully applied to the direct cellular imaging of mitochondrial GSH with a good response to varying amounts of mitochondrial GSH in cells, which is useful as a mitochondrial GSH tracker and much more superior to the commercially available thiol probe (mCB) or GSH-silent (rhodamine 123) MitoTracker. We anticipate the probe can be further served as a therapeutic reagent for mitochondrial GSH-related pathology.

dx.doi.org/10.1021/ja500962u | J. Am. Chem. Soc. 2014, 136, 7018−7025

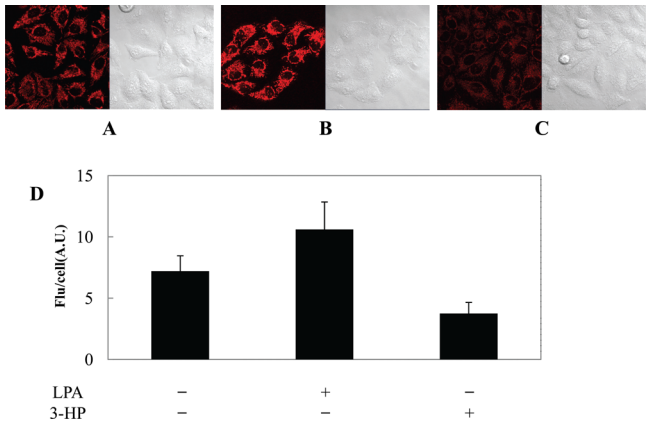

Figure 9. Confocal laser scanning microscopic images of HeLa cells by **MitoGP** (2.0 μM, 30 min, λ_{ex} 555 nm) in the presence of LPA or 3-HP. (A) **MitoGP** only, (B) **MitoGP** + LPA (1.8 mM, 24 h), (C) **MitoGP** + 3-HP (1 mM, 5 min then 2 h incubation), (D) their histograms of fluorescence intensities.

EXPERIMENTAL SECTION

General Methods. All chemicals and solvents for synthesis were purchased from commercial suppliers (Sigma-Aldrich, Fluka, Acros) and were used without further purification, unless otherwise stated. The composition of mixed solvents is given by the volume ratio (v/v). Thin layer chromatography (TLC) was performed using Merck silica gel 60 F_{254} alumina plates with a thickness of 0.25 mm. Flash column chromatography was performed on silica gel 60 (230−400 mesh ASTM; Merck). ^{1}H NMR and ^{13}C NMR spectra were recorded using Bruker 400 (400 MHz for ^{1}H, 100 MHz for ^{13}C) with chemical shifts (δ) reported in ppm relative to the solvent residual signals of $CDCl_3$ (7.16 ppm for ^{1}H, 77.16 ppm for ^{13}C), CD_3OD (3.31 ppm for ^{1}H, 49.00 ppm for ^{13}C) and coupling constants reported in Hz. High resolution mass spectra (HRMS) were obtained using a MALDI-TOF or FAB mass spectroscopy.

Synthesis of MitoGP. NaH (62 mg, 2.6 mmol) was added slowly to a solution of compound **2** (0.42 g, 1.73 mmol) in anhydrous DMF (3 mL). The mixture was stirred for 10 min, and compound **1** (1.37 g, 1.73 mmol) in DMF (2 mL) was added dropwise to the mixture. The resulting reaction mixture was stirred at room temperature for 12 h. After the reaction was complete, the solvent was removed under reduced pressure. The crude product was purified by column chromatography on silica gel using dichloromethane and methanol (10:1, v/v, R_f 0.35) as eluent, to give **MitoGP** as a dark-blue solid (1.30 g) in 75% yield.

^{1}H NMR (400 MHz, $CDCl_3$) δ 8.37 (d, ^3J = 9.2 Hz, 2H), 8.06 (d, ^3J = 9.2 Hz, 2H), 8.01 (d, ^3J = 9.2 Hz, 2H), 7.85 (d, ^3J = 14 Hz, 2H), 7.36−7.13 (m, 10H), 6.38 (d, ^3J = 14 Hz, 2H), 4.61 (t, ^3J = 6.4 Hz, 4H), 4.03 (t, ^3J = 6.8 Hz, 4H), 2.92 (t, ^3J = 6.4 Hz, 4H), 2.88 (t, ^3J = 6.0 Hz, 4H), 2.11 (q, ^3J = 6.0 Hz, 2H), 1.55 (q, ^3J = 6.8 Hz, 4H), 1.34 (s, 12H), 1.31(q, ^3J = 7.2 Hz, 4H), 0.89 (t, ^3J = 7.2 Hz, 6H). ^{13}C NMR (100 MHz, $CDCl_3$) δ 171.85, 170.91, 162.67, 162.65, 155.61, 148.58, 147.69, 141.81, 141.38, 140.79, 128.45, 126.16, 125.24, 124.73, 123.67, 123.12, 122.03, 115.43, 111.10, 101.45, 65.17, 48.95, 40.62, 32.26, 30.43, 27.93, 24.63, 21.12, 19.00, 13.64 (30 carbon peaks). HRMS (MALDI$^+$, DHB): $[M]^+$ calcd for $C_{56}H_{64}N_5O_7$, 918.4803; found, 918.4808.

Synthesis of Compound 3. **MitoGP** (100 mg, 0.100 mmol) was dissolved in anhydrous THF (3 mL), and *t*-BuONa (48 mg, 0.500 mmol) was added to the solution and stirred for 20 h at room temperature. Trifluoroacetic acid (0.076 mL, 1.00 mmol) was slowly added to the mixture, which was then stirred at room temperature for 6 h to produce a dark-green solution from the original red color. After the reaction was complete, all solvents were evaporated under reduced pressure. The crude compound was purified by silica gel column chromatography (CH_2Cl_2/CH_3OH = 10/1) to obtain compound **3** as a green solid. (63 mg, 78%).

^{1}H NMR (CD_3OD, 400 MHz): δ 8.40 (d, ^3J = 9.2 Hz, 2H), 8.11 (d, ^3J = 9.2 Hz, 2H), 8.05 (d, ^3J = 9.2 Hz, 2H), 7.97 (d, ^3J = 14 Hz, 2H), 7.37−7.16 (m, 10H), 6.40 (d, ^3J = 14 Hz, 2H), 4.38 (t, ^3J = 7.2 Hz, 4H), 2.85 (t, ^3J = 5.6 Hz, 4H), 2.62 (t, ^3J = 7.2 Hz, 4H), 2.09 (q, ^3J = 5.6 Hz, 2H), 1.37 (s, 12H). ^{13}C NMR (CD_3OD, 100 MHz): δ 176.56, 172.21, 162.95, 162.56, 155.72, 148.66, 147.78, 141.96, 141.41, 141.15, 128.35, 125.86, 124.80, 124.47, 123.03, 121.87, 121.72, 115.50, 110.83, 100.45, 48.87, 41.63, 34.91, 26.82, 23.89, 21.04. (26 carbon peaks) HRMS (MALDI$^+$, DHB): $[M]^+$ calcd for $C_{48}H_{48}N_5O_7$, 806.3554; found, 806.3550.

Synthesis of Compound 4. Compound **3** (11 mg, 14 μmol) was dissolved in anhydrous DCM (1 mL), and DCC (15 mg, 70 μmol) was added to the solution and stirred for 10 min at 0 °C. *N*-Hydroxysuccinimide (NHS, 8 mg, 70 μmol) was added to the mixture, which was stirred for 1 h at 0 °C. After monitoring the reaction by TLC, 4-(2-aminoethyl)morpholine (4 μL, 30 μmol) was added, and the solution stirred for an additional 20 min at 0 °C. After the reaction wa complete, all solvents were evaporated under reduced pressure. The crude compound was purified by silica gel column chromatography (CH_2Cl_2/CH_3OH = 10/1) to obtain compound **4** as a green solid. (5 mg, 33%).

^{1}H NMR ($CDCl_3$, 400 MHz): δ 8.39 (d, ^3J = 9.2 Hz, 2H), 8.08 (d, ^3J = 9.2 Hz, 2H), 8.03 (d, ^3J = 9.2 Hz, 2H), 7.92 (t, ^3J = 5.2 Hz, 1H), 7.88 (d, ^3J = 14 Hz, 2H), 7.38−7.15 (m, 10H), 6.34 (d, ^3J = 14 Hz, 2H), 4.47 (t, ^3J = 6.8 Hz, 4H), 3.69 (t, ^3J = 4.4 Hz, 8H), 3.40 (dt, ^3J = 6.4, 5.2 Hz, 4H), 2.87 (m, 8H), 2.54 (t, ^3J = 6.4 Hz, 4H), 2.50 (t, ^3J = 4.4 Hz, 8H), 2.10 (t, ^3J = 5.6 Hz, 2H), 1.37 (s, 12H). ^{13}C NMR ($CDCl_3$, 100 MHz): δ 171.17, 169.43, 162.64, 155.57, 148.61, 147.67, 145.43, 141.84, 141.42, 140.73, 128.90, 126.15, 125.22, 124.75, 123.92, 122.92, 121.88, 115.43, 111.21, 110.02, 66.85. 57.09, 48.95, 41.17, 36.26, 33.86, 29.70, 27.95, 24.57, 21.11. HRMS (MALDI$^+$, DHB): $[M]^+$ calcd for $C_{60}H_{72}N_9O_7$, 1030.5555; found, 1030.5530.

UV−Vis and Fluorescence Spectral Measurement. A stock solution (10 mM) of **MitoGP** in DMSO was prepared. For UV−vis spectral measurement, a sample solution was prepared by mixing an appropriate amount of the stock solution of **MitoGP** with an appropriate amount of each AA and finally diluting with HEPES buffer (0.10 M, pH 7.4) to obtain the desired concentration of **MitoGP** and AA. The fluorescence intensities of the NIR dyes were similarly measured with a slit width of 10 nm × 10 nm in medium or low mode of intensity.

Quantum Yield Measurement. IR-820 was chosen as a reference compound for determination of the quantum yields. The compound exhibits spectral properties similar to those of **MitoGP** in both absorbance and fluorescence with a maximum wavelength at 835 and 836 nm, respectively. The measurement was carried out in HEPES buffer (0.10 M, pH 7.4). Quantum yields were calculated by the comparison of the ratio between the areas under the fluorescence curve of the dyes and the reference compound. The measurements were taken at the

same absorbance intensity for both of the dyes and the reference compound at the indicated excitation wavelength.

Cellular Imaging Experiment. For the detection of GSH in live cells, HeLa cells were cultured in Dulbecco's modified Eagle's medium (DMEM) supplemented with 100 units/mL penicillin, 100 μg/mL streptomycin, and 10% heat-inactivated fetal bovine serum. The cells were seeded on a Ø 35 mm glass-bottomed dish at a density of 1×10^5 cells in a culture medium and incubated overnight in preparation for live-cell imaging by confocal laser scanning microscope (CLSM). The HeLa cells were treated with 1 or 2 μM of **MitoGP** in a serum free medium for 30 min and washed twice with prewarmed 1 × PBS before imaging by CLSM. To enhance the concentration of cellular GSH, HeLa cells were treated with α-lipoic acid (LPA, 1.8 mM) for 24 h, washed twice with prewarmed 1 × PBS buffer, and followed by **MitoGP** for 30 min before the cellular imaging experiment was performed for the live cells. In order to reduce the concentration of mitochondrial GSH, HeLa cells were treated with mitochondrial enzyme substrates, 3-hydroxy-4-pentenoate (3-HP) or 3-oxo-4-pentenoate (3-OP),[17] washed twice with prewarmed 1 × PBS buffer, and followed by **MitoGP** for 30 min before the cellular images were taken under a CLSM using the excitation channel (λ_{ex} 555 nm).

■ ASSOCIATED CONTENT

Supporting Information

Experimental details including synthesis, NMR and MS spectra. This material is available free of charge via the Internet at http://pubs.acs.org.

■ AUTHOR INFORMATION

Corresponding Author

haejkim@hufs.ac.kr

Notes

The authors declare no competing financial interest.

■ ACKNOWLEDGMENTS

This work was supported by the National Research Foundation of Korea (NRF 2011-0028456).

■ REFERENCES

(1) (a) Jocelyn, P. C. *Biochim. Biophys. Acta* **1975**, *396*, 427. (b) Wahllander, A.; Soboll, S.; Sies, H. *FEBS Lett.* **1979**, *97*, 138.

(2) (a) Guo, Z.; Park, S.; Yoon, J.; Shin, I. *Chem. Soc. Rev.* **2014**, *43*, 16. (b) Lee, M. H.; Yang, Z.; Lim, C. W.; Lee, Y. H.; Dongbang, S.; Kang, C.; Kim, J. S. *Chem. Rev.* **2013**, *113*, 5071. (c) Lim, C. S.; Masanta, G.; Kim, H. J.; Han, J. H.; Kim, M. H.; Cho, B. R. *J. Am. Chem. Soc.* **2011**, *133*, 11132. (d) Lee, M. H.; Han, J. H.; Lee, J.-H.; Choi, H. G.; Kang, C.; Kim, J. S. *J. Am. Chem. Soc.* **2012**, *134*, 17314.

(3) (a) Yang, X.; Guo, Y.; Strongin, R. M. *Angew. Chem., Int. Ed.* **2011**, *50*, 10690. (b) Wang, H.; Zhou, G.; Gai, H.; Chen, X. *Chem. Commun.* **2012**, *48*, 8341. (c) Guo, Z.; Nam, S. W.; Park, S.; Yoon, J. *Chem. Sci.* **2012**, *3*, 2760. (d) Chen, H.; Zhao, Q.; Wu, Y.; Li, F.; Yang, H.; Yi, T.; Huang, C. *Inorg. Chem.* **2007**, *46*, 11075. (e) Lee, K.-S.; Kim, T.-K.; Lee, J. H.; Kim, H.-J.; Hong, J.-I. *Chem. Commun.* **2008**, 6173.

(4) (a) Niu, L.-Y.; Guan, Y.-S.; Chen, Y.-Z.; Wu, L.-Z.; Tung, C.-H.; Yang, Q.-Z. *J. Am. Chem. Soc.* **2012**, *134*, 18928. (b) Guo, Y.; Yang, X.; Hakuna, L.; Barve, A.; Escobedo, J. O.; Lowry, M.; Strongin, R. M. *Sensors* **2012**, *12*, 5940. (c) Shao, N.; Jin, H.; Wang, H.; Zheng, J.; Yang, R.; Chan, W.; Abliz. *J. Am. Chem. Soc.* **2010**, *132*, 725.

(5) (a) Zhang, Z.; Achilefu, S. *Org. Lett.* **2004**, *6*, 2067. (b) Narayanan, N.; Patonay, G. *J. Org. Chem.* **1995**, *60*, 2391.

(6) IR-820 as a reference compound, ε at 835 nm = 1.2×10^5 M^{-1} cm^{-1}, Φ 0.034 in DMSO, ex 720 nm. Berezin, M. Y.; Lee, H.; Akers, W.; Achilefu, S. *Biophys. J.* **2007**, *93*, 2892.

(7) (a) Ogawa, M.; Kosaka, N.; Choyke, P. L.; Kobayashi, H. *Cancer Res.* **2009**, *69*, 1268. (b) Tan, X.; Luo, S.; Wang, D.; Su, Y.; Cheng, T.; Shi, C. *Biomaterials* **2012**, *33*, 2230.

(8) A complex between **MitoGP** and ethanolamine showed a similar blue shift fluorescence maximum at 756 nm (Figure S21 in the SI), which was generally observable by the fluorophores with amino-substituted heptamethine dye: (a) Yang, Z.; Lee, J. H.; Jeon, H. M.; Han, J. H.; Park, N.; He, Y.; Lee, H.; Hong, K. S.; Kang, C.; Kim, J. S. *J. Am. Chem. Soc.* **2013**, *135*, 11657. (b) Kiyose, K.; Aizawa, S.; Sasaki, E.; Kojima, H.; Hanaoka, K.; Terai, T.; Urano, Y.; Nagano, T. *Chem.—Eur. J.* **2009**, *15*, 9191.

(9) It is noteworthy that 1:1 complex formation between **MitoGP** and Cys or Hcy in the fluorescence spectral conditions is assumed due to the very low concentration of probes at micromolar concentration and excess amount of Cys/Hcy (Figure S12 in the SI), as compared to 2:1 complex condition (Figure S13 in the SI).

(10) The nitro group usually acts as a fluorescence quencher. We adopted the nitroazo group as a quencher because its extinction coefficient is high enough to cause effective quenching of the NIR fluorescence of **MitoGP**. (a) Wang, R.; Yu, F.; Chen, L.; Wang, L.; Zhang, W. *Chem. Commun.* **2012**, *48*, 11757. (b) Han, M.; Hara, M. *J. Am. Chem. Soc.* **2005**, *127*, 10951. (c) Rau, H. *Angew. Chem., Int. Ed.* **1972**, *12*, 224.

(11) We observed that the UV−vis spectra of **MitoGP** in a HEPES buffer displayed ratiometric changes together with a bathochromic shift ($\Delta\lambda$ = + 10 nm) at its maximum wavelength probably due to *J*-aggregation. The original spectra of **MitoGP** were rapidly recovered in the presence of a surfactant such as cetyltrimethylammonium bromide, indicating that a reversible reaction of vesicle or micelle-to-monomer transition took place with **MitoGP**. Refer to the examples of *J*-aggregation of cyanine dyes: (a) Vaidyanathan, S.; Patterson, L. K.; Möbius, D.; Gruniger, H. R. *J. Phys. Chem.* **1985**, *89*, 491. (b) Rotermund, F.; Weigand, R.; Holzer, W.; Wittmann, M.; Penzkofer, A. *J. Photochem. Photobiol. A: Chem.* **1997**, *110*, 75.

(12) (a) Zhang, C.; Spokoyny, A. M.; Zou, Y.; Simon, M. D.; Pentelute, B. L. *Angew. Chem., Int. Ed.* **2013**, *52*, 14001. (b) Gragg, J. L. *M.S. Thesis*, Georgia State University, 2010, GA.

(13) Strekowski, L.; Lipowska, M.; Patonay, G. *J. Org. Chem.* **1992**, *57*, 4578.

(14) 3-HP is expected to be metabolized by the mitochondrial specific enzyme (3-hydroxybutanoate dehydrogenase) to 3-OP, which subsequently reacts with GSH and thereby depletes mitochondrial GSH in cells. (a) Shan, X.; Jones, D. P.; Hashmi, M.; Anders, M. W. *Chem. Res. Toxicol.* **1993**, *6*, 75. (b) Lluis, J. M.; Morales, A.; Blasco, C.; Colell, A.; Mari, M.; Garcia-Ruiz, C.; Fernandez-Checa, J. C. *J. Biol. Chem.* **2005**, *280*, 3224.

(15) Due to the cytotoxic effect of 3-OP (Figure S20 in the SI), we prefer 3-HP as a mitochondrial GSH scavenger in cells.

(16) (a) Packer, L. *Drug. Metab. Rev.* **1998**, *30*, 245. (b) Packer, L.; Tritschler, H. J.; Wessel, L. *Free Radical Biol. Med.* **1997**, *22*, 359.

(17) Zibuck, R.; Streber, J. M. *J. Org. Chem.* **1986**, *54*, 4717.